Molecular Crystals and Liquid Crystals
Publication details, including instructions for authors and subscription information:
http://www.tandfonline.com/loi/gmcl20

Permittivity of Chiral Smectics in the Broad Range from 0.1 mHz to 50 kHz: Discovery of Sub-mHz Dielectric Dispersion

Evgeny Pozhidaev [a], Fernando C. M. Freire [b c], Cesar Augusto Refosco Yednak [b c d], Alfredo Strigazzi [c], Sofia Torgova [a c], Vadim Molkin [a] & Maxim Minchenko [a]

[a] P.N. Lebedev Physical Institute, Russian Academy of Sciences, Leninsky Prospect, Moscow, Russia

[b] Dep. de Fisica, Universidade Estadual de Maringá, Avenida Colombo, Maringá, Paraná, Brasil

[c] Dip. di Fisica and CNISM, Politecnico di Torino, Corso Duca degli Abruzzi, Torino, Italy

[d] Universidade Tecnológica Federal do Paraná, Campus Pato Branco, Via do Conhecimento, Pato Branco, Paraná, Brasil

Version of record first published: 16 Jun 2011

To cite this article: Evgeny Pozhidaev, Fernando C. M. Freire, Cesar Augusto Refosco Yednak, Alfredo Strigazzi, Sofia Torgova, Vadim Molkin & Maxim Minchenko (2011): Permittivity of Chiral Smectics in the Broad Range from 0.1 mHz to 50 kHz: Discovery of Sub-mHz Dielectric Dispersion, Molecular Crystals and Liquid Crystals, 546:1, 186/[1656]-194/[1664]

To link to this article: http://dx.doi.org/10.1080/15421406.2011.571151

Mol. Cryst. Liq. Cryst., Vol. 546: pp. 186/[1656]–194/[1664], 2011

ISSN: 1542-1406 print/1563-5287 online
DOI: 10.1080/15421406.2011.571151

Permittivity of Chiral Smectics in the Broad Range from 0.1 mHz to 50 kHz: Discovery of Sub-mHz Dielectric Dispersion

EVGENY POZHIDAEV,[1] FERNANDO C. M. FREIRE,[2,3] CESAR AUGUSTO REFOSCO YEDNAK,[2,3,4] ALFREDO STRIGAZZI,[3] SOFIA TORGOVA,[1,3] VADIM MOLKIN,[1] AND MAXIM MINCHENKO[1]

[1]P.N. Lebedev Physical Institute, Russian Academy of Sciences, Leninsky Prospect, Moscow, Russia
[2]Dep. de Fisica, Universidade Estadual de Maringá, Avenida Colombo, Maringá, Paraná, Brasil
[3]Dip. di Fisica and CNISM, Politecnico di Torino, Corso Duca degli Abruzzi, Torino, Italy
[4]Universidade Tecnológica Federal do Paraná, Campus Pato Branco, Via do Conhecimento, Pato Branco, Paraná, Brasil

Dielectric dispersion of a chiral smectic liquid crystal has been measured in the very broad frequency range from 0.1 mHz to 50 kHz. Two regions of dispersion have been recognized: the first one, from 0.1 mHz to 0.1 Hz was for the first time measured, the second one, from 100 Hz to 50 kHz, which is known as mainly due to Goldstone mode, has been confirmed.

Keywords Chiral smectic liquid crystal; dielectric dispersion; dielectric susceptibility; Goldstone mode; permittivity

1. Introduction

According to experimental data reported in the literature [1–7], the typical relaxation frequency of the helix of a chiral smectic ferroelectric liquid crystal (FLC) is 10^2–10^3 Hz. The previous authors proved the existence of only one of such relaxation frequency, directly measuring the real part of the permittivity. Instead, other authors [8,9] investigating dielectric losses have found additional lower characteristic frequency, about 10 Hz [8] and 30 mHz [9].

We planned to analyze the FLC dielectric behavior, detecting the real part of the permittivity in a more broad frequency range as compared with former data, in order to clarify the appearance of the low frequency mode of FLC helix relaxation. Here

Address correspondence to Alfredo Strigazzi, Dip. di Fisica and CNISM, Politecnico di Torino, Corso Duca degli Abruzzi 24, I-10129, Torino, Italy. Tel.: +39-564 73 34; Fax: +39-564 73 99; E-mail: alfredo.strigazzi@polito.it

we announce the result of our investigation, showing experimentally that the low frequency relaxation of the helical structure occurs in a very low frequency range (0.1 mHz–0.1 Hz). Usually, dielectric dispersion detection for describing collective modes is carried out from 5 Hz to 100 kHz. The lower limit comes from the fact that ordinary dielectric spectroscopy instruments giving the real part of the permittivity are reliable from 5 Hz up; whereas the upper limits depends on the fact that above 100 kHz only intra-molecular modes take place [10,11].

We were interested to overcome the lower limit for the observation of the permittivity real part even in comparison with instruments like Solatron-1250 analyzer (which resolves 10^{-2} Hz): to this purpose a special technique for very low frequency dielectric measurements (down to 10^{-4} Hz) has been developed. The features of this method will be described below, and the experimental results will be discussed as well.

2. Experimental

2.1. *Materials*

Asymmetric boundary conditions were used for manufacturing of FLC cell [12,13]. In this approach only one indium tin oxide (ITO) surface of a FLC cell was covered with a polyimide layer with structure of repeating pyromellitic dianhydride (PMDA) and 4,4′-oxidianiline (ODA) units, which after imidization has the structure shown in Figure 1, whereas another one was simply washed in *N,N*-dimethyl formamide (DMF) and covered with 4.8 μm calibrated spacers. The polyimide solution was spin-coated onto ITO electrode, dried at 180°C during 1 hour and cured at 290°C during 1 hour. The aligning layer thickness turns out to be 10 nm; the layer was rubbed with a piece of lawn.

It is important to note that the aligning layer texture is not continuous, but island-like, which is a consequence of the polyimide solution flow at spin-coating on ITO rough surface: the polyimide areas with thickness about 10 nm (black color) fill the valleys among ITO peaks (white color, height of peaks is about 15–20 nm) [14,15] – see Figure 2.

Such a broken aligning layer ensures conductivity of electronic kind prohibiting charge accumulation between liquid crystal and the polyimide.

The spin coating deposit of polyimide has been done with the aim of ensuring perfect planar alignment of FLC molecules [16]. The cell was filled by capillarity with the sample in isotropic phase. The sample consists of the chiral smectic FLC with commercial name NS-1010. Such a mixture exhibits at room temperature ferrielectric behavior; and its helix pitch $p_o = 450$ nm is definitely smaller than the FLC layer thickness d. The ohmic conductivity of the sample is $10^{-9}\,\mathrm{S \cdot m^{-1}}$: this means that

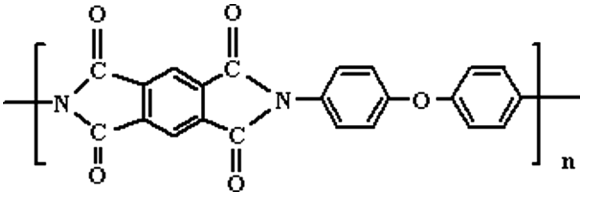

Figure 1. Structure formula of polyimide used as spin coating layer on one cell glass plate.

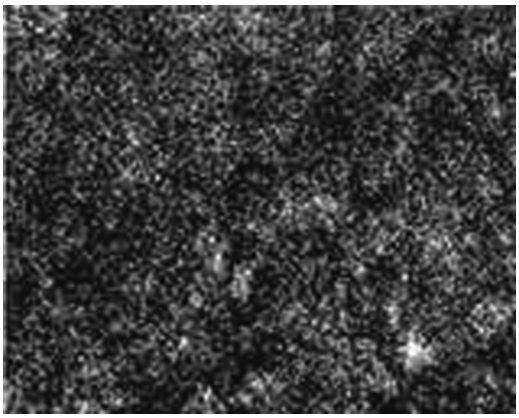

Figure 2. Island structure of polyimide aligning layer with thickness around 10 nm, made with electronic microscope Quanta 600 F. Size of the picture is $200 \times 160\,\mathrm{nm}^2$.

it is a dielectric material. The spontaneous polarization P_s of the sample is $9 \cdot 10^{-4}$ $\mathrm{C/m}^2$, as measured by us. The cell size is given by the thickness $d = 4.8\,\mu\mathrm{m}$ and by the capacitor frontal area $S = 1.69\,\mathrm{cm}^2$. The boundary conditions imply that the FLC helix axis is parallel to the cell plates.

2.2. *Methods*

We present a method for measuring the dielectric susceptibility χ of a cell filled with a low conducting liquid through the detection of the characteristic cycle $I(V_{\mathrm{cell}})$, where I is the current passing trough the sample cell due to the application of a periodic voltage V_{cell}. We are interested to consider the FLC sample, which is practically non-conducting one, and to detect the real part of the permittivity in a very broad frequency range, from 10^{-4} to 10^5 Hz. Thus it was necessary to plan two slightly different procedures, the first one suitable for the lower frequency interval (10^{-4}–10^{-1} Hz) and the second for the higher frequency interval (10^{-1} Hz–40 kHz): hence two different experimental set-up have been established. In both cases, a triangular-in-time voltage $V(t)$ at fixed frequency is applied to the cell.

In the first set–up (see Fig. 3) the function generator supplies the voltage V_{FG} to a simple circuit formed by a calibrated standard resistance R_{o} in series with the sample cell. Minimum noise was reached in the experiment at $R_{\mathrm{o}} = 1\,\mathrm{M\Omega}$. The voltage amplitude V_{cell} onto the cell was kept as $V_{\mathrm{cell}} \ll V_{\mathrm{th}}$, where V_{th} is the critical threshold voltage for the helix unwinding, which value is greater than 1 V at all frequencies, as it has been measured in our laboratories. In fact the function generator voltage was fixed at $V_{\mathrm{FG}} = \pm 0.5\,\mathrm{V}$; and the cell voltage turned out to be close to the same value. The first set-up refers to lower frequency measurements (10^{-4}–10^{-1} Hz). Since for very low frequency the detection of one cycle implies hours of measurements, the cell has to be put inside a box controlling the thermal variation for a long time with accuracy of about 1°C. The two parameters $V_{\mathrm{FG}}(t)$, $V_{\mathrm{o}}(t)$ are detected as a function of time with rate of 1 reading/s, by means of two very sensitive ($1{:}10^8$) Agilent multimeters, driven by a computer via LabView software especially implemented to be applied to this method.

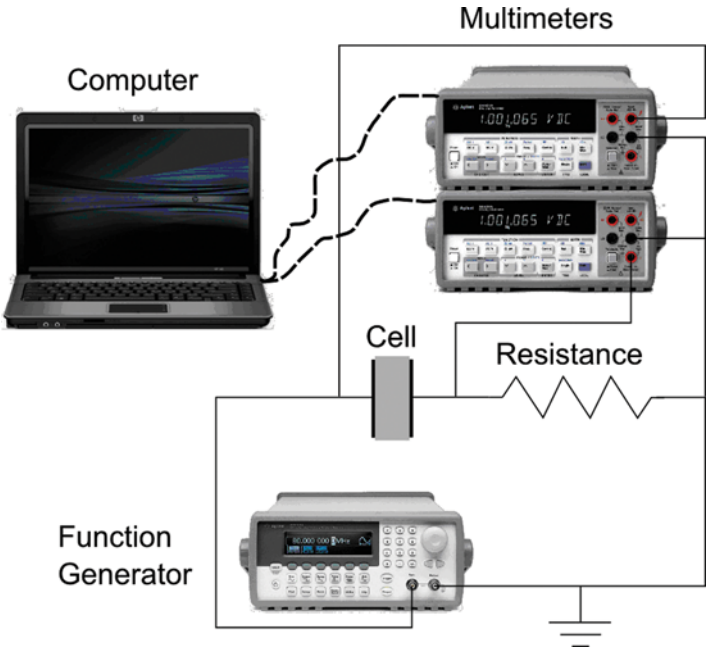

Figure 3. Scheme of low frequencies detection circuit: the function generator supplies a triangular-in-time voltage at low frequency, from 0.1 to 100 mHz. The multimeters measure the potential on the standard resistance ($V_0 = R_0^* I$) and the one determined by the function generator (V_{FG}), respectively. The computer drives the detection runs by means of LabView program and automatically collect the multimeters data via GPIB interface. Then the correct V_{cell} is only indirectly measured, as ($V_{FG} - R_0^* I$). (Figure appears in color online.)

The second set up is represented in Figure 4. It is relevant to higher frequency measurements (10^{-1}Hz–50 kHz). Here the constraint concerning temperature stability is less hard, but the fact that one cycle duration is smaller than 10 s at maximum and smaller than $5 \cdot 10^{-4}$ s for the highest frequency requires recording by an

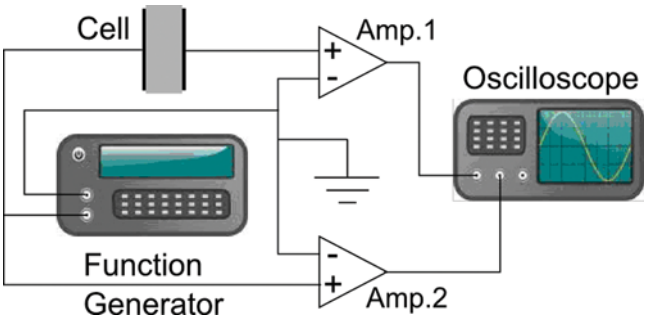

Figure 4. Scheme of middle frequencies (from 0.1 Hz to 50 kHz) detection circuit: the Function Generator supplies a ramp potential of variable frequency to the cell. The amplifiers send to the oscilloscope the signals current – voltage applied the cell. The maximum potential and the current are detected once per single frequency value. (Figure appears in color online.)

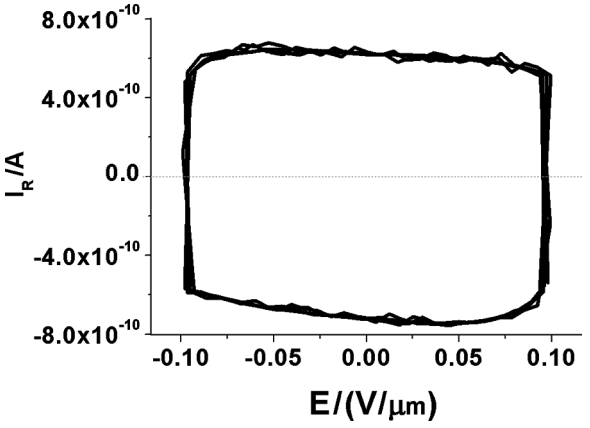

Figure 5. Quasi-rectangular hysteretic free cycle of the polarization reversal current I_R measured at frequency $f = 10^{-2}$ Hz with a cell 4.8 μm thick, with frontal active surface $S = 1.69\,cm^2$, filled by the chiral smectic – ferrielectric mixture NS-1010 with helix pitch $p_0 = 450$ nm.

oscilloscope. Here the valuable signals $V_{FG}(t)$, $V_{cell}(t)$ are directly sent to the two channels of the oscilloscope by means of two amplifiers.

2.3. *Data*

By applying the voltage for $3 \div 5$ cycles duration we directly detect a well repeatable hysteretic free cycle $I(V_{cell})$, having a quasi-parallelogram shape, were the inclined sides take into account the residual presence of ions, giving the small real current contribution. From the first elaboration of the experimental data a quasi-rectangular cycle is obtained, expressed by the two horizontal sides crossing the previous cycle at $V_{cell} = 0$, defining the polarization reversal current I_R. (for a typical picture, see Fig. 5). It has to be noted that I_R does not depend on the field $E(t)$ but only on its maximum value E_o.

The original data provide the total current I passing through the cell at $V_{cell} = 0$ as a function of frequency in 9 decades, from 0.1 mHz to 50 kHz. Such a limit current I is by definition depurated by the ohmic contribution, but is determined by two sources, the high frequency asymptotic behavior and the Goldstone mode. In Figure 6 the trend of $I(f)$ is reported.

3. Results and Discussion

3.1. *Evaluation of Dielectric Susceptibility*

The dielectric susceptibility χ vs. frequency f can be obtained from the experimental data concerning the total current $I(f)$ according to the following relationship

$$\chi(E) = \frac{1}{4\varepsilon_o} I(f, E_o) S^{-1} f^{-1} E_o^{-1} - 1 \tag{1}$$

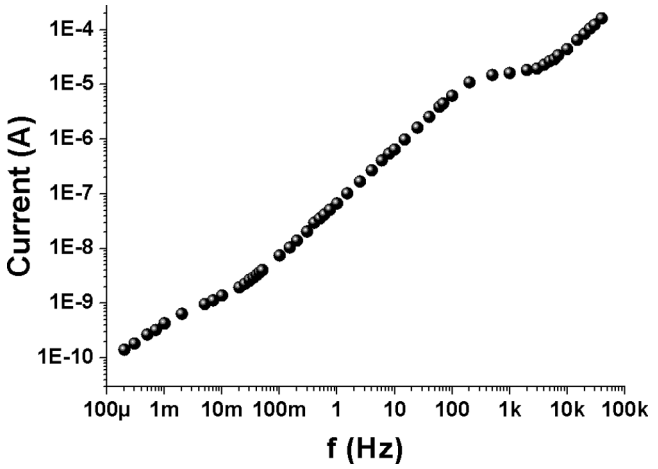

Figure 6. Picture of total current I at $V_{cell} = 0$ vs. frequency f, including high frequency contribution. Measurements have been done at 23°C.

where ε_o is the vacuum permittivity, and E_o is the electric field amplitude applied to the cell (see Fig. 7).

3.2. *Analysis of Susceptibility Dispersion*

First of all let us note that the last term present in Eq. (1) is negligible practically in all frequency interval, except at higher frequency, above 2 kHz (at 2 kHz the dielectric susceptibility is 23, then the relative permittivity $\varepsilon_r = 24$, hence assuming $\varepsilon_r \sim \chi$ implies to insert a maximum inaccuracy about 4%). Furthermore, in order to depurate χ from the asymptotic high frequency contribution χ_∞, it would be necessary to

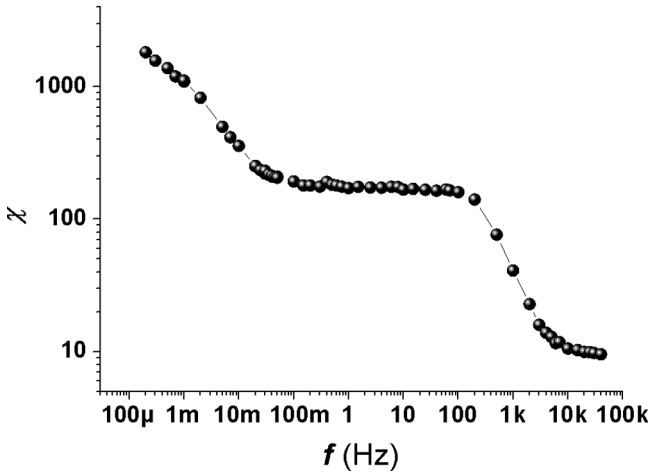

Figure 7. Picture of total dielectric susceptibility χ vs. frequency f, including high frequency contribution. The curve is obtained from data of Figure 6 according to relationship (1).

reach the right side plateau, then to implement detection to MHz range: but here we can only estimate the situation. All usual dielectric isotropic liquid materials exhibit about $\chi_\infty \sim 5$; in the present case $\chi(50\,\text{kHz}) = 9.5$: hence $5 \leq \chi_\infty \leq 9.5$ is expected for the FLC sample.

With the aim of depurating the data from the high frequency contribution, characteristic of a usual isotropic liquid, let us consider the susceptance $B \equiv 2\pi f C$, where C is the capacitance of the cell: Since the cell admittance Y of a pure dielectric material coincides with B, we have that the ohmic part I_o of the current is proportional to the product $(f\varepsilon_r)$. As a result, taking into account equation (1), we obtain that $\chi_o = \chi_\infty$ is independent of the frequency, as it is well known for an ordinary isotropic liquid. As a conclusion, from Figure 7 it is possible to plot the susceptibility of ordered structure $\chi_s = \chi - \chi_o$ simply transferring the position of f axis by χ_∞ up. If we neglect this operation, just by posing $\chi = \chi_s$, in the frequency range below 100 Hz, where $\chi = 160$, we insert a maximum inaccuracy about 6%, which is vanishing by reducing the frequency (at $f = 0.1$ mHz the χ inaccuracy is 0.05%).

Now, considering the behavior of χ over all 9 decades, it can be seen that Figure 7 shows clearly two dispersion regions separated by a plateau, the first one from 0.1 mHz to 100 mHz, the second one from 100 Hz to 50 kHz. The latter is well known, and mainly corresponds to Goldstone mode dispersion [1–7] biased by the asymptotic high frequency contribution. The plateau is relevant to the static dielectric susceptibility χ_G of Goldstone mode accounted with the same bias. As it is known [18], χ_G is expressed as:

$$\chi_G = \frac{P_s^2}{2\varepsilon_0 K \theta^2 q_0^2} \tag{2}$$

where θ is the molecular tilt angle in smectic layers, K is the elastic modulus of the helical structure in one elastic constant approximation and $q_0 = 2\pi/p_0$ is the wave vector of the helix. Taking into account the parameters P_s, p_0, $\theta = 32^\circ$, $\chi_G = 160$ measured by us in the frequency range 0.1 Hz ÷ 100 Hz, and the relationship (2), we evaluated the elastic modulus for NS-1010: $K = 4.7 \cdot 10^{-12}$ N, which is the same order of magnitude as the usual values of the elastic constant of nematic liquid crystals. According to our data, which we will published in another paper, this is typical for esters composed chiral smectics. On the other hand, our former evaluations of the same modulus but for another smectic liquid crystal FLC-579 based on phenyl – and biphenyl – pyrimidines, developed in P.N. Lebedev Physical Institute of Russian Academy of Sciences, gave $K = 2.4 \cdot 10^{-11}$ N [19]. That means that the range of K value variation dependent on chemical structure in smectic liquid crystals is considerably more broad in comparison with nematic liquid crystals.

The range at lower frequency appears to be the most interesting, due to the fact that it clearly evidences a definite dispersion not reaching any left side plateau even downwards to 0.1 mHz. The reason of such a behavior is still under question. For sure it cannot be due to ions collected between ITO layer and aligning layer, as claimed both in ref [8] for the dielectric dispersion detected about 10 Hz and in ref [9]. for the dielectric dispersion detected about 10 mHz, discussing dielectric losses measurements: in fact, in the present case the aligning layer is broken due to island texture, and this prevents any charge coupling at the interface.

We suggest that the dielectric dispersion discovered by us could be due to many sources, f.i.:

1. the Goldstone mode, more favored by a quasi-stationary application of the cell voltage;
2. the arising of soliton-like waves, due to larger relaxation time in the helix deformation [20];
3. the possible appearance of a domain-ordered texture, due to slightly difference of the in-plane orientation of the helix axis;
4. the possible coupling between the two boundary surfaces, due to the different boundary strength (the so called "thickness mode") [21,22].

Note that also the not complete blocking character of the electrodes, providing charge injection even at very small voltage is here excluded, since already the ohmic contribution has been cancelled.

4. Conclusions and Perspectives

In this paper dielectric measurements vs. frequency over 9 decades have been performed, detecting current – voltage histeretic free cycles, and obtaining the dielectric susceptibility curve. The results clearly show two dispersion regions separated by a plateau, the first one from 0.1 mHz to 100 mHz, the second one from 100 Hz to 50 kHz. The dielectric dispersion in the range 0.1 mHz–10 mHz was discovered by us, whereas the higher frequency behavior reported in the literature has been confirmed. The sample elastic constant has been indirectly measured, and compared with the one of other chiral FCL material. Conjectures about possible explanation of low frequency dispersion have been suggested: their impact will be investigated in a further paper.

Acknowledgment

This work was supported by Russian Foundation of Basic Research (RFBR), Grants 09-03-12234-ofi_m, 09-03-12263-ofi_m, 10-02-01336-a, 10-03-13305-PT_omi, 10-03-90016-Bel_a, 08-02-01074-a, by Russian Federal Agency of Science and Innovations (project 02.740.11.5166). F.C.M. Freire acknowledges grant from Conselho Nacional de Desenvolvimento Cientifico e Tecnologico, Brazil (CNPq), from Associazione per lo Sviluppo Scientifico e Tecnologico del Piemonte (ASP) and is grateful to Organizers of XXIII ILCC Krakow and to Politecnico di Torino, Dipartimento di Fisica, for support. Thanks are due to M. Becchi for preliminary measurements, and to E. S. Kuz'menko, A. A. Zhukov for providing electronic microscope photo.

References

[1] Ostrovskii, B. I., Rabinovich, A. Z., Sonin, A. S., Strukov, B. A., & Chernova, N. I. (1977). *Jetp. Lett.*, *25*, 70.
[2] Hoffmann, I., Kuczynski, W., & Maleski, I. (1978). *Mol. Cryst. Liq. Cryst.*, *44*, 287.
[3] Levstik, A., Zheks, B., Levstik, I., Blinc, R., & Filipic, C. (1979). *J. Phys. Colloq.*, *40*, C300.
[4] Benguigui, L. (1982). *Physique, J.*, *43*, 915.

[5] Levstik, A., Kutnjak, Z., Filipic, C., Levstik, I., Zheks, B., & Carlsson, T. (1991). *Ferroelectrics*, *113*, 207.
[6] Gouda, F., Skarp, K., & Lagerwall, S. T. (1991). *Ferroelectrics*, *113*, 165.
[7] Ganzke, D. (2002). *Untersuchungen an ausgewählten Flussigkristall – Systemen, Dissertation zur Erlangung des akademischen Grades eines Doctor-Ingenieurs*, Darmstadt: Deutschland.
[8] Havriliak, S., Vij, J. K., & Ming, N. (1999). *Liq. Cryst.*, *26*, 465.
[9] Biradar, A. M., Killian, D., Wrobel, S., & Haase, W. (2000). *Liq. Crys.*, *27*, 225.
[10] Carlsson, T., Zeks, B., Filipic, C., & Levstik, A. (1990). *Phys. Rev. A*, *42*, 877.
[11] Merino, S., De Daran, F., De La Fuente, M. R., Perez Jubindo, M. A., & Sierra, T. (1997). *Liq. Cryst.*, *23*, 275.
[12] Pozhidaev, E., Chigrinov, V., Huang, D., Zhukov, A., Ho, J., & Kwok, H. S. (2004). *Jap. Journ. App. Phys.*, *43*, 5440.
[13] Kiselev, A. D., Chigrinov, V. G., & Pozhidaev, E. P. (2007). *Phys. Rev. E 75*, 061706.
[14] Pozhidaev, E. P., Zhukov, A. A., Chigrinov, V. G., Kompanets, I. N., Gukasjan, E. E., Komarov, P. S., Bobilev, Yu. P., Shoshin, V. M., Andreev, A. L., Kwok, H. S., Torgova, S. I., & Strigazzi, A. (2006). *Proc. Int. Disp. Res. Conf. (IDRC'06)*, Kent, September 18–20.
[15] Kuz'menko, E. S., Zhukov, A. A., Pozhidaev, E. P., & Kompanets, I. N. (2010). *Nanotechn. in Russia*, *5*, 123.
[16] Zhukov, A. A., Pozhidaev, E. P., Bakulin, A. A., & Babaevski, P. G. (2006). *Cryst. Rep.*, *51*, 680.
[17] Pozhidaev, E., Andreev, A., & Kompanets, I. (1995). *Proc. SPIE*, *2731*, 100.
[18] Urbanc, B., Zheksh, B., & Carlsson, T. (1991). *Ferroelectrics*, *113*, 219.
[19] Pozhidaev, E., Torgova, S., Minchenko, M., Yednak, R. C. A., Strigazzi, A., & Miraldi, E. (2010). *Liq. Cryst.*, *37*, 1067.
[20] Tsoy, E. N., Stewart, I. W., & Abdullaev, F. Kh. (1999). *Phys. Rev. E*, *60*, 5568.
[21] Glogarova, M., Sverenyak, H., Holakovsky, J., Nguen, H. T., & Destrade, C. (1995). *Mol. Cryst. Liq. Cryst.*, *263*, 245.
[22] Novotna, V., Glogarova, M., Bubnov, A. M., & Sverenyak, H. (1997). *Liq. Cryst.*, *23*, 511.